A Kinetic Study on the Influence of Nucleoside Triphosphate Effectors on Subunit Interaction in Mouse Ribonucleotide Reductase†

Rolf Ingemarson* and Lars Thelander

Department of Medical Biochemistry and Biophysics, Umeå University, S-901 87 Umeå, Sweden

Received January 25, 1996; Revised Manuscript Received April 11, 1996⊗

ABSTRACT: For enzymatic activity, mouse ribonucleotide reductase must form a heterodimeric complex composed of homodimeric R1 and R2 proteins. Both substrate specificity and overall activity are regulated by the allosteric effectors ATP, dATP, dTTP, and dGTP, which bind to two different sites found on R1, the activity site and the substrate specificity site. We have used biosensor technique to directly observe the effects of these nucleotides on R1/R2 interactions. In the absence of effectors, positive cooperativity was observed with a Hill coefficient of 1.8 and a K_D of 0.5 μM. In the presence of dTTP or dGTP, there was no cooperativity and subunit interaction was observed at a much lower R1 concentration. The highest R1/R2 affinity was in the presence of dATP or ATP with K_Ds of 0.05−0.1 μM. In all experiments, the molar stoichiometry between the subunits was close to 1:1. Our data support a model whereby binding of any of the effectors to the substrate specificity site promotes formation of the R1 dimer, which we believe is prerequisite for binding to the R2 dimer. Additional binding of either ATP (a positive effector) or dATP (a negative effector) to the activity site further increases R1/R2 association. We propose that binding of ATP or dATP to the activity site controls enzyme activity, not by changing the aggregation state of the R1/R2 proteins as proposed earlier, but rather by locally influencing the long range electron transport between the catalytic site of R1 and the tyrosyl free radical of R2.

Ribonucleotide reductase catalyzes the first unique step in the metabolic reactions leading to DNA synthesis. The enzyme reduces the ribonucleotides CDP, ADP, GDP, and UDP to the corresponding deoxyribonucleotides (Thelander & Reichard, 1979; Eriksson & Sjöberg, 1989; Stubbe, 1990; Reichard, 1993).

The active form of the mammalian ribonucleotide reductase, which belongs to the class I ribonucleotide reductases like the extensively studied *Escherichia coli* enzyme, is composed of two nonidentical homodimeric subunits, proteins R1 and R2. Each polypeptide of the R2 subunit contains a binuclear non-heme ferric center which, during its formation, generates a tyrosyl free radical, essential for activity (Thelander & Gräslund, 1994). The R1 subunit contains substrate binding sites and binding sites for allosteric effectors as well as redox active disulfides participating in the reduction.

The interaction between the subunits of mammalian ribonucleotide reductase is dependent on the C-terminal seven amino acid residues of the R2 protein (Yang et al., 1990; Cosentino et al., 1991). This C-terminal part is flexible in isolated protein R2 in solution, but after binding to the R1 subunit, it becomes rigid and structured (Lycksell et al., 1994). Subunit interaction in ribonucleotide reductase from many different species has been shown to be dependent on the unique C-terminal tail of the R2 protein (Dutia et al., 1986; Cohen et al., 1986; Climent et al., 1991; Filatov et al., 1992). *In vivo* active specific inhibitors, mimicking the herpes simplex virus R2 C-terminal peptide, were developed against the viral ribonucleotide reductase (Krogsrud et al., 1993; Liuzzi et al.,1994). Affinity labeling the mouse protein R1 with photoreactive mouse R2 C-terminal heptapeptides localized the R2 interaction area to the C-terminal region of the R1 protein (Davis et al., 1994).

To supply the cell with balanced pools of deoxyribonucleotides, the mammalian enzyme is allosterically controlled. Four different nucleoside triphosphates, ATP, dTTP, dGTP, and dATP, have been shown to regulate enzyme activity. The presence of an allosteric effector is required to observe any measurable enzymatic activity from the mammalian ribonucleotide reductase (Eriksson et al., 1979). The mammalian R1 subunit contains two different classes of binding sites for allosteric effectors. The positive effector ATP and the negative effector dATP compete for one class of allosteric binding sites that regulates the overall activity of the enzyme. All four effectors ATP, dATP, dTTP, and dGTP, bind to the other class of allosteric sites regulating the substrate specificity (Eriksson et al., 1979; Thelander et al., 1980; Reichard, 1993). Although qualitatively correct, we believe that the earlier reported number of effector binding sites per mammalian R1 polypeptide should be reconsidered (Thelander et al., 1980). The presence of two different classes of allosteric effector binding sites in the mammalian R1 protein is supported by the characterization of separate mutations in the activity and specificity sites (Eriksson et al., 1981a,b). The allosteric regulation of mammalian ribonucleotide reductase is summarized in Table 1.

The influence of allosteric effectors on the mammalian R1 protein in the absence of the R2 protein has been studied earlier using the calf thymus protein and glycerol gradient centrifugations. The R1 protein in the absence of effectors

† This research was supported by grants from the Swedish Natural Science Research Council, Cancerfonden, Magn. Bergvalls Stiftelse, Fonden för medicinsk forskning, and Lion's Research Foundation, Umeå University.

* To whom correspondence should be addressed. Tel +46 90 16 53 64; Fax +46 90 13 63 10; E-mail roling@panther.cmb.umu.se.

⊗ Abstract published in *Advance ACS Abstracts,* June 1, 1996.

S0006-2960(96)00184-5 CCC: $12.00

Table 1: Allosteric Regulation of Mammalian Ribonucleotide Reductase

effector at specificity site	effector at activity site	stimulates the reduction of	inhibits the reduction of
ATP	ATP	CDP, UDP	GDP, ADP
dTTP	ATP	GDP	CDP, UDP, ADP
dGTP	ATP	ADP	CDP, UDP, GDP
dATP	dATP		CDP, GDP, UDP, ADP

sedimented as a double peak, indicating a mixture of monomeric and dimeric protein. In the presence of dTTP, protein R1 sedimented as a dimer, and in the presence of dATP the protein sedimented as a tetramer. In ATP, the protein sedimented as a mixture of dimers and tetramers (Engström et al., 1979; Thelander et al., 1980). This demonstrates that the aggregation behavior of the mammalian R1 protein is strongly influenced by the allosteric effectors.

The influence of allosteric effectors on the *E. coli* ribonucleotide reductase has earlier been studied by ultracentrifugation (Brown & Reichard, 1969a,b ; Thelander, 1973). The bacteriophage T4 ribonucleotide reductase was reported to contain more tightly bound R1 and R2 subunits than the *E. coli* enzyme (Berglund, 1972). However, this tight binding was recently demonstrated by immunoprecipitation to be completely dependent on the presence of either of the four allosteric effectors (Hanson & Mathews, 1994).

The recently presented crystal structure of the *E. coli* R1 protein showed that polypeptide interactions are weak with a narrow interaction area mainly formed by two α-helixes. However, there are also a number of flexible loops of weak density which may stabilize dimer formation in the holoenzyme. One effector binding site—most probably the specificity site—was suggested to be very close to the dimer interaction area (Uhlin & Eklund, 1994).

Here we report for the first time a quantitative description of the influence of the allosteric effectors on the binding between the R1 and R2 proteins using the mouse ribonucleotide reductase and the BIAcore biosensor technique. This technique allows direct observation of protein−protein interaction in real time and determination of the different kinetic binding constants. The data presented here, along with previous data derived from enzyme activity measurements, glycerol gradient results, and crystal structure analyses, allow us to put forth a unifying model describing the influence of the allosteric effectors on ribonucleotide reductase holoenzyme formation.

EXPERIMENTAL PROCEDURES

Biosensor Analysis. Subunit interaction was studied by biosensor analysis using the Pharmacia Biosensor (BIAcore) method (Jönsson et al., 1991; Malmquist, 1993). The immobilization of protein R2 to the dextran layer on the sensor chip was according to the amino coupling method as previously described (Rova et al., 1995). After activation of the dextran layer, 30 μL of protein R2 at a concentration of 0.4 mg/mL (4.4 μM of dimeric protein) or alternatively 0.1 mg/mL (1.1 μM) in 50 mM phosphate buffer, pH 7.0, was injected at a flow rate of 5 μL/min. The R1 protein was equilibrated with the running buffer (10 mM Hepes, 0.15 M NaCl, 10 mM $MgCl_2$, 1 mM EDTA, 0.05% (v/v) Surfactant P20 (Pharmacia Biosensor), pH 7.4, and allosteric effector as indicated) by gel filtration on a Sephadex G 25

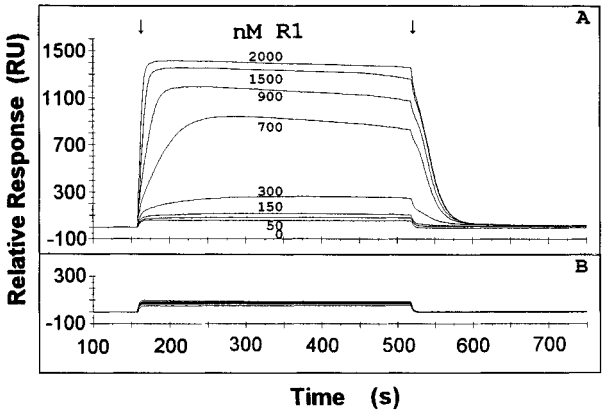

FIGURE 1: (A) Overlay of sensorgrams showing the interaction between immobilized protein R2 (900 RU) and increasing concentrations of mobile phase protein R1 (0, 50, 150, 300, 700, 900, 1500, and 2000 nM). The first arrow from the left indicates injection of protein R1 (association phase). The second arrow shows when R1 injection is interrupted and bound protein starts to wash away by the running buffer (dissociation phase). In this figure, the bulk effect response of 50 −100 RU was not subtracted, indicated by the initial rapid drop during the dissociation phase (see Experimental Procedures). (B) Control where no protein R2 was immobilized. Increasing concentrations of protein R1 (0−2000 nM) are injected.

column, and before injection, dithiothreitol was added to 2 mM final concentration. In the experiments with 5 mM ATP, the $MgCl_2$ concentration was raised to 15 mM to be in excess over ATP. Protein R1 was normally injected as a series of six to nine concentrations between 50 nM of dimeric protein (9 μg/μL) and 2000 nM (360 μg/μL), in both the presence and absence of allosteric effectors (nucleotides were purchased from Pharmacia Biotech). In some experiments the maximal R1 concentration was 3600 nM (650 μg/μL). Between each injection bound R1 protein was removed by washing with 0.5 M KCl. The interactions were studied at a constant temperature of 22 °C. The resonance unit (RU) is proportional to the mass, and 1 RU corresponds to a surface concentration of 1 pg of protein/mm^2 of the 100 nm thick dextran layer (Jönsson et al., 1991).

Determination of Equilibrium Dissociation Constants. From a series of increasing concentrations of protein R1 in the mobile phase, the levels of the relative response were measured when the interaction had reached equilibrium. A Scatchard plot was used to determine the dissociation equilibrium constant from these data. The general Scatchard equation is $B/F = (1/K_D) \times (B_{max} - B)$. B represents the amount of bound protein R1 per immobilized protein R2 determined when the interaction had reached equilibrium. A low, gradual decrease in binding was observed at equilibrium in some experiments in the absence of effectors (Figure 1). In these experiments, B was measured from the baseline to the highest equilibrium level. The value of the response at equilibrium (R_{eq}), measured in resonance units (RU) was divided with the relative response obtained from the immobilization of protein R2. The number gives the weight ratio between bound protein R1 and immobilized protein R2. Using the molecular mass for dimeric protein R1 and R2 (2 × 90 kDa and 2 × 45 kDa, respectively), the molar ratio of bound protein R1 to immobilized protein R2 was calculated [$B = R_{eq}/\{$(immobil R2) × (2 × 90)/(2 × 45)$\}$]. F represents free ligand (concentration of injected protein R1). The flow of protein R1 was constant, and therefore the concentration of the injected protein R1 is set

equal to free protein R1 in these calculations—maximally 1.6 ng of protein was bound and the minimal amount of injected protein was 85 ng. Bound R1 over R2/Free R1 (B/F) was plotted against bound R1 over R2 (B). The negative value of the slope of the Scatchard plot gives the association equilibrium constant (K_A). The dissociation equilibrium constant K_D is $1/K_A$. The maximal amount of bound protein R1 per mole immobilized protein R2 (B_{max}) was calculated from the intercept with the abscissa. For all concentrations of protein R1, a control sample was injected in a flow cell lacking immobilized protein R2. The response arising from a small bulk effect from 50 to 100 resonance units was subtracted from the interaction response.

Determination of the Hill Coefficient. The Hill coefficient gives the number of different binding steps in an interaction and measures the degree of cooperativity (Bennet, 1978). The Hill equation applied for these experiments is $\log(R_{eq}/(R_{max} - R_{eq})) = n \log [F] - \log K_D'$, where n is the Hill coefficient, F is the concentration of injected free ligand (protein R1), and K_D' is a composite constant composed of the intrinsic dissociation constant K_D and interaction factors that determine the degree to which K_D is altered at each discrete binding step. R_{eq} is the response at equilibrium measured in resonance units (RU), and R_{max} is the maximal response measured in resonance units (RU). The Hill coefficient (n) was determined from the slope of the line obtained from a plot of $\log(R_{eq}/(R_{max} - R_{eq}))$ against $\log F$ (Bennet, 1978).

Determination of the Association Rate Constants. The association rate constant was determined from a series of solutions containing increasing concentrations of protein R1 interacting with immobilized protein R2. Using the BIAcore software, the association rate constant was determined from the equation $dR/dt = k_{assoc} \times F(R_{max} - R) - k_{dissoc} \times R$. The derivative of the response dR/dt from the association phase was plotted against the response R for different concentrations of the R1 protein. Thereafter, the slope of each line (k_s) was determined from the linear section of each curve. The k_s value was plotted against the concentration (F) of free protein R1. The association rate constant k_{assoc} could finally be calculated from the slope of the new plot according to the equation $k_s = -k_{assoc} \times F + k_{dissoc}$ (cf. Karlsson et al., 1991; Rova et al., 1995).

Determination of the Dissociation Rate Constant. The dissociation rate constant was determined from two time points in the early phase of dissociation. The derivative of the response curve reflects the dissociation rate in the equation $dR/dt = -k_{dissoc} \times R$. Integration of the equation with respect to time gives the equation $\ln(R_{t_1}/R_{t_n}) = k_{dissoc} \times (t_n - t_1)$. A plot of $\ln(R_{t_1}/R_{t_n})$ vs time $(t_n - t_1)$ gives a value of the dissociation rate (k_{dissoc}) from the slope, where R_{t_1} is the response at an arbitrary start time t_1 and R_{t_n} is the response at a subsequent time t_n. This estimation of k_{dissoc} is valid under the assumption that rebinding of released ligand is negligible, i.e., the ligand is efficiently removed by the buffer flow (Karlsson et al., 1991).

Expression, Purification, and Determination of the Concentration of Proteins R1 and R2. Recombinant mouse R1 and R2 proteins were expressed in *E. coli* bacteria using a pET 3a expression vector (Studier et al., 1990) and purified as described earlier (Davis et al., 1994; Studier et al., 1990). Protein R1 and R2 concentrations were measured by light absorbance at 280 nm using the extinction coefficients $E^{1\%}_{1cm}$ (280 nm) 12.0 (Thelander et al., 1980) and $E^{1\%}_{1cm}$ (280−310 nm) 13.8 (Mann et al., 1991), respectively.

RESULTS

Immobilization of Protein R2 and General Design of the R1/R2 Binding Experiments. Protein R2 was immobilized to a sensor chip as described in Experimental Procedures. The immobilization of protein R2 at a concentration of 4.4 μM gave an increase of 1000 resonance units (RU), which corresponds to 1 ng/mm^2 (Jönsson et al., 1991) or 11.1 fmol/mm^2, while a concentration of 1.1 μM gave an increase of 500 RU. With a surface of 0.8 mm^2, 1000 RU corresponds to a total of 0.8 ng of bound protein R2 or 8.9 fmol. During the immobilization, a total of 12 μg of protein R2 was injected. This low degree of attachment (only 0.007%) makes it unlikely that the protein is attached at multiple binding sites and therefore increases the chance that it is attached in an active form.

The interaction between the R1 and R2 subunits was studied in real time. With the injection of protein R1 at 160 s after the start of plotting the sensorgram (Figure 1), the association phase starts immediately, reaching an equilibrium plateau R_{eq} at time points between 170 and 450 s depending on the R1 concentration, where higher concentrations reach equilibrium faster than lower concentrations. At the time point 530 s in the sensorgram, the injection of protein R1 was interrupted and followed by running buffer alone, and this starts the dissociation phase (Figure 1).

A series of solutions containing increasing concentrations of protein R1 was injected to the same sensor chip with immobilized protein R2. Between each injection, the sensor chip was regenerated by washing with 0.5 M KCl which removed all bound protein R1. The results from such an experiment are shown in Figure 1. This "overlay plot" demonstrates that increasing concentrations of protein R1 resulted in increasing equilibrium levels. The equilibrium levels were approaching asymptotically a maximal value R_{max}, which is set by the number of available binding sites on the immobilized protein R2. In a control experiment with the same series of increasing concentrations of protein R1 passing the sensor chip without immobilized protein R2, a "bulk effect" gave a response of only 50−100 RU (Figure 1B).

The immobilized protein R2 showed the same capacity with respect to protein R1 binding for periods of up to 3 days. Repeated injections of a constant amount of protein R1 in the presence of dATP (see below) resulted in a maximal loss of binding capacity of 6%. Only in the presence of high concentrations of ATP did we see an appreciable decrease in R2 binding capacity (see below).

Analysis of the Binding in the Absence and Presence of Effectors. A completely diverse pattern of binding in the absence and in the presence of the four effectors dATP, dTTP, dGTP, and ATP is illustrated by plotting the response at equilibrium (R_{eq}) against the concentration of the injected protein R1 in a dose response curve (Figure 2). In the absence of allosteric effectors, a much higher concentration of protein R1 was required to detect binding and the curve had a sigmoid shape. Such a curve suggests that the binding is cooperative.

The negative allosteric effector dATP was most efficient in increasing the affinity between the R1 and R2 subunits.

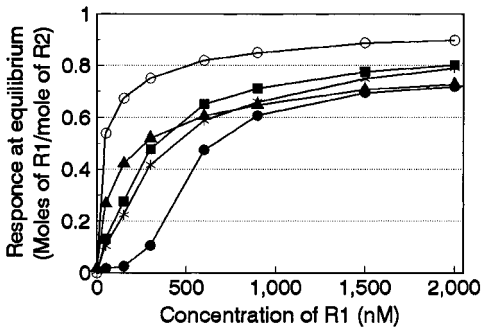

FIGURE 2: Dose−response curve where the response at equilibrium is plotted against the concentration of protein R1 in the absence of effector (the same data as shown in Figure 1) (●), in the presence of 100 μM dATP (○), in the presence of 100 μM dTTP (∗), in the presence of 100 μM dGTP (■), or in the presence of 5 mM ATP (▲). Bound protein R1 is given as moles of R1 per mole of immobilized R2 (Experimental Procedures).

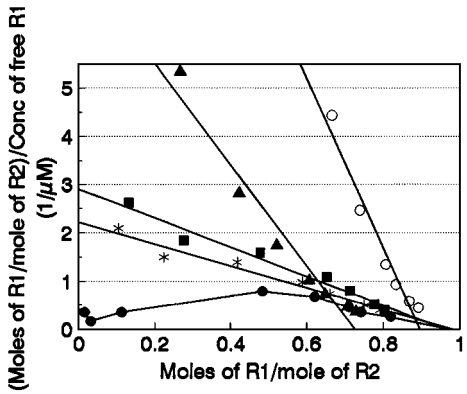

FIGURE 3: Scatchard plot of the response at equilibrium of increasing concentrations of protein R1 interacting with a constant amount of immobilized protein R2. No effector present (●), in the presence of 100 μM dATP (○), 100 μM dTTP (∗), 100 μM dGTP (■), or in the presence of 5 mM ATP (▲). The experimental values are the same as the ones analyzed in Figure 2.

This effect is most clearly seen at low concentrations of protein R1. The dose response curve in the presence of dATP followed a hyperbolic pattern (Figure 2). The results with the positive effector ATP were similar to the results with dATP in the initial part of the curve, but the values never reached the same levels as with dATP. A lower molar stoichiometry was often obtained in the presence of ATP compared to the other effectors (Figures 2 and 3). This is most likely due to gradual inactivation of the immobilized protein R2 in the presence of high concentrations of ATP. When the first injection on a freshly prepared R2 sensor chip contained the highest R1 concentration, 0.9 mol of R1 bound per mole of R2 also in the presence of ATP. The R2 inactivation seemed to originate from impurities in the ATP preparation and was less pronounced with highly purified ATP. The intracellular concentrations of ATP are much higher than the concentrations of the dNTPs, and therefore we used 5 mM ATP. This concentration gives maximal stimulation of pyrimidine ribonucleotide reduction (Eriksson et al., 1979).

The effects on R1/R2 binding of the GDP reduction specific effector dTTP were less pronounced than the dATP/ATP effects. However, also dTTP markedly increased the affinity between proteins R1 and R2, and the curve followed a similar hyperbolic shape as with dATP (Figure 2). The ADP reduction specific effector dGTP gave results almost identical to the ones obtained with dTTP.

Determination of the R1/R2 Equilibrium Dissociation Constants in the Absence and in the Presence of Effectors. To determine the equilibrium dissociation constant K_D = [R1][R2]/[R1R2] for the interaction between the R1 and R2 subunits of mouse ribonucleotide reductase, the equilibrium response data from increasing concentrations of protein R1 as described above were analyzed in a Scatchard plot (cf. Experimental Procedures).

With no effector present during the experiment, several phases of binding seemed to occur. Instead of a straight line, the plot resulted in a curve with a positive slope at low concentrations of protein R1 and a negative slope at higher concentrations (Figure 3). This again suggested positive cooperativity for the R1/R2 binding in the absence of effectors. Choosing only the four last points of the curve for regression analysis gave an approximate K_D of 0.5 μM. Another series of measurements with higher concentrations of protein R1 (up to 3600 nM) was made for a more accurate estimation of the K_D value. These experiments confirmed the first estimated K_D value of 0.5 μM (data not shown).

In the presence of dATP, the slope of the line in the Scatchard plot of Figure 3 was steeper than without effector, indicating a lower K_D value. The equilibrium dissociation constant K_D was decreased from 0.5 μM in the absence of effector to 0.05 μM in the presence of 100 μM dATP (Table 2). In the presence of dATP all points could be plotted on a straight line with no signs of cooperativity as seen in the absence of effector (Figure 3).

The effects of dTTP and dGTP on the R1/R2 binding were also analyzed in the same Scatchard plot (Figure 3). In the presence of 100 μM dTTP or 100 μM dGTP, estimation of the equilibrium dissociation constant from the linear curves in Figure 3 gave K_D values around 0.4 μM (Table 2). These values were in the same range or slightly lower then the K_D in the absence of effector, but in the latter case the concentration of protein R1 had to be much higher to get a linear curve for the K_D estimation.

Finally, we studied the effects of ATP. The slope of the linear ATP curve in the Scatchard plot of Figure 3 is similar to the slope seen with dATP giving a K_D of 0.12 μM (Table 2).

Stoichiometry of the R1/R2 Binding. Binding of the R1 subunit to immobilized protein R2 occurred with the same stoichiometry without effector as in the presence of the nucleoside triphosphates dTTP, dGTP, dATP, or ATP. Values between 0.72 and 0.98 mol of R1/mol of R2 were obtained from the intercept with the abscissa in the Scatchard plot (Figure 3).

Quantification of Cooperativity in Binding. To quantify the cooperativity in binding seen in the absence of effectors, a series of data from the same type of experiments as in Figure 3 was analyzed in a Hill plot (Figure 4). The Hill coefficient for R1/R2 binding without effector was determined to 1.8 (Table 2). This should be compared to a Hill coefficient of 1 in the presence of effectors confirming the lack of cooperativity with the effectors present.

Kinetic Constants of R1/R2 Association and Dissociation. A separate analysis of the association phase in the reaction R1 + R2 → R1/R2 according to the method described in the Experimental Procedures gave reproducibly a high association rate constant k_{assoc} of about 500 000 $(M\ s)^{-1}$ in the presence of dATP or ATP (Table 2). In the absence of effector, the association rate constant was only around

Table 2: Summary of Binding Constants Characterizing the Interaction between Mouse Protein R1 ± Allosteric Effectors and Immobilized Mouse Protein R2, Measured by Biosensor Technique

	equilibrium dissociation constant: K_D (μM)	association rate constant: $10^{-6} \times k_{assoc}$ ($M^{-1}\,s^{-1}$)	dissociation rate constant: k_{dissoc} (s^{-1})	Hill coeff
R2 + R1	0.52 ± 0.20[a]	0.16 ± 0.04[a]	0.055 ± 0.009	1.8
R2 + R1 + dTTP	0.46 ± 0.31	0.34 ± 0.12[a]	0.045 ± 0.010	1.0
R2 + R1 + dGTP	0.40 ± 0.31	0.36 ± 0.11[a]	0.045 ± 0.009	1.0
R2 + R1 + dATP	0.05 ± 0.02	0.56 ± 0.06	nd (0.028)[b]	1.0
R2 + R1 + ATP	0.12 ± 0.04	0.47 ± 0.07	nd (0.056)[b]	1.0

[a] Points at low protein R1 concentrations omitted in the calculation. [b] No direct measurements could be made. These values are estimated from the K_D and k_{assoc} values.

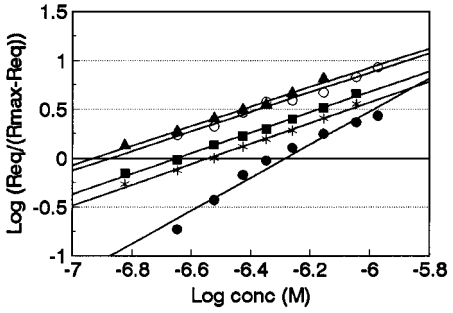

FIGURE 4: Hill plot of the R1/R2 interaction ± effectors. The Hill equation applied for this experiment is $\log(R_{eq}/(R_{max} - R_{eq})) = n \log F - \log K_D'$ (see Experimental Procedures). The Hill coefficient (n) was determined from the slope of the line. Increasing concentrations of protein R1 (50−1060 nM) were interacting with a constant amount of immobilized protein R2. No effector present (●), in the presence of 50 μM dATP (○), in the presence of 50 μM dTTP (∗), in the presence of 50 μM dGTP (■), or in the presence of 1 mM ATP (▲).

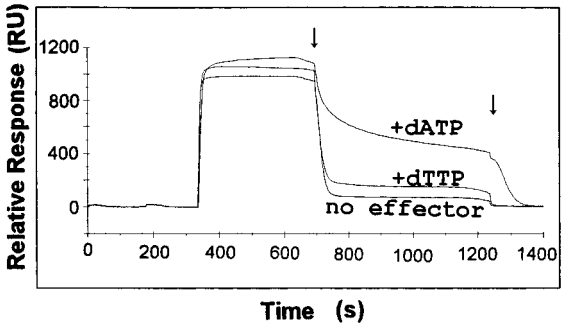

FIGURE 5: Sensorgrams of protein R1 interacting with immobilized protein R2 in the absence of effector, in the presence of 100 μM dTTP or in the presence of 100 μM dATP. The injection of protein R1 stopped at the time point 710 s indicated by the first arrow from the left and effectors were removed from the running buffer at the time point 1210 s indicated by the second arrow.

150 000 $(M\,s)^{-1}$, while the values in the presence of dTTP or dGTP were in between these values (Table 2). There were two different slopes of the plot k_s versus C (see Experimental Procedures) used for the determination of the association rate constants in the absence of effector and with dTTP or dGTP. Therefore, in the calculations of the data obtained in the absence of effectors, only the values obtained from the 3−5 measurements with the highest protein R1 concentrations were used, while in the presence of dTTP or dGTP, the 5−7 values with the highest R1 concentrations were used.

A dissociation rate constant of 0.04−0.05 s^{-1} was obtained from plots of $\ln(R_{t_1}/R_{t_n})$ versus time (Experimental Procedures) both in the absence of effector and in the presence of dTTP or dGTP (Table 2). No estimation was made in the presence of ATP or dATP since the dissociation did not go to completion during the measured time interval. After a relatively fast initial dissociation, the dissociation in the presence of ATP/dATP became extremely slow at approximately half the equilibrium level. Therefore, the dissociation plots $\ln(R_{t_1}/R_{t_n})$ versus time did not follow a linear pattern. Most likely, this is due to rapid rebinding of dissociated protein R1 in the presence of ATP/dATP. This interpretation is supported by the dissociation curve in Figure 5where the dATP present in the running buffer during the first part of the dissociation phase was then removed from the running buffer. This immediately resulted in a fast dissociation. The effect was the same with ATP (data not shown) but hardly noticeable with dTTP (Figure 5).

The accuracy of the two rate constants obtained in the absence of effectors could be estimated by calculating the equilibrium dissociation constant (K_D) from the equation $K_D = k_{dissoc}/k_{assoc}$. This calculation gave K_D values of 0.53−0.23 μM, which is within the range of the directly determined K_D (Table 2).

DISCUSSION

Glycerol gradient centrifugations, gel filtration experiments, analytical ultracentrifugations (Thelander et al., 1980, 1985), and the crystal structure[1] show that the mammalian R2 polypeptides form very tightly bound homodimers. Therefore, they are most likely immobilized in the form of dimers on the sensor chip. In contrast, the mammalian R1 polypeptides alone in solution occur mainly as monomers in the absence of effectors, as indicated by glycerol gradient centrifugations (Thelander et al., 1980). Photoaffinity labeling experiments with the *E. coli* R1 protein using dTTP and the recently elucidated crystal structure of the same *E. coli* protein suggest that the allosteric effector binding site determining the specificity is located very close to the domain of interaction between the R1 polypeptides (Eriksson et al., 1986; Uhlin & Eklund, 1994). This is also very close to the substrate binding site, which may allow local interactions between substrate and effector. Interestingly, a similar positioning of an allosteric binding site close to the substrate binding site was recently observed for the glutamine-5-phosphoribosyl-1-pyrophosphate amidotransferase enzyme catalyzing the committed step in purine biosynthesis (Smith et al., 1994).

The location of the allosteric effector binding site determining the activity has not been determined in the bacterial enzyme. However, a G-to-A transition at codon 57, changing an Asp to an Asn, made the mouse R1 protein resistant to negative feedback regulation by dATP. This indicates that the activity site is located in the amino-terminal region of

[1] B. Kauppi et al., manuscript in preparation.

the R1 protein (Caras & Martin, 1988). In the crystal structure of the *E. coli* R1 protein, this position corresponds to one of the α-helices supposed to be in close contact to the R2 protein in the R1/R2 complex (Uhlin & Eklund, 1994).

In our experiments, similar slopes in the Scatchard plots were obtained at high concentrations of protein R1 alone or at low R1 concentrations in the presence of dTTP or dGTP. This indicates that a major effect of these allosteric effectors could be to increase dimerization of the R1 monomers. This is in agreement with the finding that the specificity site is located close to the R1 dimer interaction area. Binding to the specificity site may induce conformation changes resulting in increased dimer formation. Furthermore, a positive cooperativity in R1/R2 binding is only observed in the absence of effectors with increasing concentrations of protein R1. This would be expected to increase the formation of R1 dimers. Our model to explain these data would be that protein R1 monomers have low affinity for the R2 protein dimer. However, once the R1 dimer is formed, it binds with high affinity to the R2 dimer.

This model may explain the effects on R1/R2 complex formation on binding allosteric effectors to the specificity site. However, the affinity between proteins R1 and R2 are much higher in the presence of ATP/dATP than in the presence of dTTP/dGTP. This may be a result of simultaneous binding of effectors to the specificity site and the activity site, a property unique to ATP or dATP. Binding to the activity site occurs secondary to binding to the specificity site due to lower affinity, at least for dATP in the *E. coli* R1 protein (Brown & Reichard, 1969b). Activity site binding may further increase R1 dimer formation or—considering the position of the activity site at the R1/R2 interface—more likely increase the affinity between the R1 and R2 dimers. The latter resembles the situation for the monomeric *Lactobacillus leichmannii* ribonucleotide reductase where the presence of allosteric effectors increases the affinity for the cobalamin coenzyme (Thelander & Reichard, 1979).

A molar stoichiometry close to 0.9:1 was obtained when protein R1 bound to immobilized protein R2. Assuming that the active native enzyme forms a complex of the $\alpha_2\beta_2$ type, an assumption supported by data from ultracentrifugation experiments (Engström et al., 1979; Thelander et al., 1980), nearly all protein R2 was immobilized in an active form. This 1:1 binding between R1 and R2 was observed both in the absence and in the presence of effectors. The 1:1 stoichiometry in the binding between R1 and R2 is an indication that immobilization of protein R2 to a surface did not seriously affect the interaction.

Considering the very similar effects on R1/R2 complex formation of the positive effector ATP and the negative effector dATP, one may ask how ATP induces an active enzyme while dATP induces an inactive form. The control must be exclusively by binding to the activity site since both ATP and dATP induce the same pyrimidine specific enzyme when bound to the specificity site as demonstrated by the D57N mutant mouse R1 protein (Caras & Martin, 1988). Earlier data suggested that enzyme activity may be controlled by an ATP/dATP induced change in the aggregation status of the R1/R2 proteins (Brown & Reichard, 1969a; Thelander, 1973). However, our data give no support for such a model. Instead, the position of the allosteric activity site in protein R1 suggests another mechanism. From the crystal structure of the *E. coli* R1 protein, this position may be located close to an essential, amino acid residue specific, long range electron transfer pathway leading from the catalytic site in R1 to the tyrosyl free radical in protein R2 (Uhlin & Eklund, 1994; Nordlund et al., 1990). This pathway is supposed to generate a transient thiyl radical in the catalytic site required for enzyme activity (Mao et al., 1992). We would like to suggest that dATP binding to the allosteric activity site blocks this long range electron transport much in the same way as substituting the conserved tryptophan 103 at the surface of protein R2 by tyrosine or phenylalanine which results in an inactive enzyme complex (Rova et al., 1995). In contrast, ATP binding to the allosteric activity site would promote electron transport.

The dissociation constant for the *E. coli* ribonucleotide reductase R1/R2 complex was reported to be 0.09−0.18 μM in the presence of 1.5 mM ATP and at 37 °C. The constant was calculated from enzymatic assays where the concentrations of protein R2 were varied while the concentration of protein R1 was kept constant (Climent et al., 1991, 1992). A comparison with the K_D value of 0.12 μM for the mouse R1/R2 interaction determined in the presence of 5 mM ATP and at 22 °C shows that the affinity between the R1 and R2 proteins is similar for the two species.

The dissociation constant clearly does not fully illustrate the influence of the allosteric effectors on R1/R2 binding. This is better illustrated by the dose response curves (Figure 2) where the interaction is studied over the full range of protein R1 concentrations since the influence of allosteric effectors is most clearly seen at lower concentrations. These low concentration points had to be excluded from the calculations of K_D.

The maximal association rate constant was obtained in the presence of dATP/ATP and was repeatedly determined to 450 000−550 000 $(Ms)^{-1}$. Under these conditions, both the activity and the substrate specificity allosteric effector sites should be fully occupied. This value may reflect the physiological relevant association rate constant. At very low protein R1 concentrations in the presence of dTTP alone, the monomer/dimer equilibrium may not be fully shifted to the dimer formation. Therefore, the association rate constant in the presence of dTTP increased with increasing protein concentrations (data not shown). However, inside a cell, protein R1 may never bind dTTP or dGTP alone but always in combination with ATP at the allosteric activity site (Eriksson et al., 1979). The dissociation rate constant showed only small changes in the absence of effector or in the presence of dTTP or dGTP with values near 0.05 s^{-1}. Notable was that the dissociation rate constant could not be directly measured in the presence of dATP/ATP since the plots of $\ln(R_{t_1}/R_{t_n})$ versus time were not linear. We think this reflects the very high association rate constant resulting in reassociation of dissociated protein. For comparison, the k_{dissoc} values in the presence of ATP and dATP were calculated from the equation $k_{dissoc} = K_D \times k_{assoc}$ which gave k_{dissoc} of 0.06 s^{-1} and 0.03 s^{-1}, respectively (Table 2). However, using the same method to calculate k_{dissoc} in the absence of effectors or in the presence of dGTP or dTTP resulted in values higher than the ones determined directly. Therefore, the calculated k_{dissoc} values for ATP or dATP may be overestimated.

Decreasing the amounts of immobilized protein R2 from 1000 to 500 RU gave no change in the estimated association

rate constants (data not shown). Therefore, we believe that we really studied the association rate without influence of the diffusion rate for protein R1 from the bulk flow to the immobilized protein R2.

To be able to unequivocally distinguish the effects of nucleotide binding to the allosteric activity sites from binding to the allosteric specificity sites, we are now in the process of expressing recombinant mouse R1 proteins having independent mutations in each of these sites.

REFERENCES

Bennett, J. P. (1978) In *Neurotransmittor receptor binding* (Yamamura, H. I., Enna, S. J., & Kuhar, M. J., Eds.) pp 57−90, Raven Press, New York.

Berglund, O. (1972) *J. Biol.Chem. 247*, 7270−7275.

Brown, N. C., & Reichard, P. (1969a) *J. Mol. Biol. 46*, 25−38.

Brown, N. C., & Reichard, P. (1969b) *J. Mol. Biol. 46*, 39−55.

Caras, I. W., & Martin, D. W. (1988) *Mol. Cell. Biol. 8*, 2698−2704.

Climent, I., Sjöberg, B. M., & Huang, C. Y. (1991) *Biochemistry 30*, 5164−5171.

Climent, I., Sjöberg, B. M., & Huang, C. Y. (1992) *Biochemistry 31*, 4801−4807.

Cohen, E. A., Gaudreau, P., Brazeau, P., & Langelier, Y. (1986) *Nature 321*, 441−443.

Cosentino, G., Lavallée, P., Rakhit, S., Plante, R., Gaudette, Y., Lawetz, C., Whitehead, P. W., Duceppe, J. S., Lépine-Frenette, C., Dansereau, N., Guilbault, C., Langelier, Y., Gaudreau, P., Thelander, L., & Guindon, Y. (1991) *Biochem. Cell Biol. 69*, 79−83.

Davis, R., Thelander, M., Mann, G., Behravan, G., Soucy, F., Beaulieu P., Lavallée, P., Gräslund, A., & Thelander, L. (1994) *J. Biol.Chem. 269*, 23171−23176.

Dutia, B. M., Frame, M. C., Subak-Sharpe, J. H., Clark, W. N., & Marsden, H. S. (1986) *Nature 321*, 439−441.

Engström, Y., Eriksson, S., Thelander, L., & Åkerman, M.(1979) *Biochemistry 18*, 2941−2947.

Eriksson, S., & Sjöberg, B. M. (1989) in *Allosteric Enzymes* (Hervé, G., Ed.) pp 189−215, CRC Press, Boca Raton, FL.

Eriksson, S., Thelander, L., & Åkerman, M. (1979) *Biochemistry 18*, 2948−2952.

Eriksson, S., Gudas, L. J., Ullman, B., Clift, S. M., & Martin, D. W.(1981a) *J. Biol. Chem. 256*, 10184−10188.

Eriksson, S., Gudas, L. J., Clift, S. M., Ullman, B., & Martin, D. W. (1981b) *J. Biol. Chem. 256*, 10193−10197.

Eriksson, S., Sjöberg, B.-M., Jörnvall, H., & Carlquist, M.(1986) *J. Biol. Chem. 261*, 1878−1882.

Filatov, D., Ingemarson, R., Gräslund, A., & Thelander, L. (1992) *J. Biol. Chem. 267*, 15816−15822.

Hanson, E., & Mathews, C. K. (1994) *J. Biol. Chem. 269*, 30999−31005.

Jönsson, U., Fägerstam, L., Ivarsson, B., Johnsson, B., Karlsson, R., Lundh, K., Löfås, S., Persson, B., Roos, H., Rönnberg, I., Sjölander, S., Stenberg, E., Ståhlberg, R., Urbaniczky, C., Östlin, H., & Malmqvist, M. (1991) *Biotechniques 11*, 620−627.

Karlsson, R., Michaelsson, A., & Mattson, L. (1991) *J. Immunol. Methods 145*, 229−246.

Krogsrud, R. L., Welchner, E., Scouten, E., & Liuzzi, M.(1993) *Anal. Biochem. 213*, 386−394.

Liuzzi, M., Déziel, R., Moss, N., Beaulieu, P., Bonneau, A-M., Bousquet, C., Chafouleas, J. G., Garneau, M., Jaramillo J., Krogsrud, R. L., Lagacé, L., McCollum, R. S., Nawoort, S., & Guindon, Y. (1994) *Nature 372*, 695−698.

Lycksell, P.-O., Ingemarson, R., Davis, R., Gräslund, A., & Thelander, L. (1994) *Biochemistry 33*, 2838−2842.

Malmqvist, M. (1993) *Nature 361*, 186−187.

Mann, G. J., Gräslund, A., Ochiai, E.-I., Ingemarson, R., & Thelander, L. (1991) *Biochemistry 30*, 1939−1947.

Mao, S., Yu, G. X., Chalfoun, D., & Stubbe, J. (1992) *Biochemistry 31*, 9752−9759.

Nordlund, P., Sjöberg, B.-M., & Eklund, H. (1990) *Nature 345*, 593−598.

Reichard, P. (1993) *Science 260*, 1773−1777.

Rova, U., Goodtzova, K., Ingemarson, R., Behravan, G., Gräslund A., & Thelander, L. (1995) *Biochemistry 34*, 4267−4275.

Smith, J. L., Zaluzec, E. J., Wery, J. P., Niu, L., Switzer, R. L., Zalkin, H., & Satow, Y. (1994) *Science 264*, 1427−1433.

Stubbe, J. (1990) *Adv. Enzymol. 63*, 349−419.

Studier, F. W., Rosenberg, A. H., Dunn, J. J., & Dubendorff, J. W. (1990) *Methods Enzymol. 185*, 60−89.

Thelander, L. (1973) *J. Biol.Chem. 248*, 4591−4601.

Thelander, L., & Reichard, P. (1979) *Annu. Rev. Biochem. 48*, 133−158.

Thelander, L., & Gräslund, A. (1994) in *Metal Ions in Biological Systems* (Sigel, H., Ed.) Vol 30 (4), pp 109−129, Marcel Dekker, New York.

Thelander, L., Eriksson, S., & Åkerman, M. (1980) *J. Biol. Chem. 255*, 7426−7432.

Thelander, M., Gräslund, A., & Thelander, L. (1985) *J. Biol. Chem. 260*, 2737−2741.

Uhlin, U., & Eklund, H. (1994) *Nature 370*, 533−539.

Yang, F. D., Spanevello, R. A., Celiker, I., Hirschmann, R., Rubin, H., and Cooperman, B. S. (1990) *FEBS Lett. 272*, 61−64.

BI960184N